BJP British Journal of Pharmacology

DOI:10.1111/j.1476-5381.2012.02230.x
www.brjpharmacol.org

RESEARCH PAPER

Azaindole derivatives are inhibitors of microtubule dynamics, with anti-cancer and anti-angiogenic activities

Renaud Prudent[1,2]*, Émilie Vassal-Stermann[2]*, Chi-Hung Nguyen[3], Marjorie Mollaret[2], Jean Viallet[1], Agnès Desroches-Castan[4], Anne Martinez[1], Caroline Barette[2], Catherine Pillet[2], Glaucio Valdameri[5], Emmanuelle Soleilhac[2], Attilio Di Pietro[5], Jean-Jacques Feige[4], Marc Billaud[1], Jean-Claude Florent[6] and Laurence Lafanechère[1,2]

[1]*Institut Albert Bonniot, CRI INSERM/UJF U823, La Tronche Cedex, France,* [2]*CEA, DSV, iRTSV/CMBA, Grenoble, France,* [3]*UMR 176 CNRS-Institut Curie, Institut Curie Bât 110, Orsay, France,* [4]*INSERM, Unit 1036, Biology of Cancer and Infection, Grenoble, France,* [5]*Equipe Labellisée Ligue 2009, Institut de Biologie et Chimie des Protéines FR 3302, BM2SI UMR 5086 CNRS/Université Lyon 1, Lyon, France, and* [6]*UMR 176 CNRS-Institut Curie, Centre de Recherche, Paris, France*

Correspondence
Laurence Lafanechère, Equipe 3 'Polarité, Développement et Cancer', Institut Albert Bonniot, Rond Point de la Chantourne, 38700 La Tronche, France. E-mail: laurence.lafanechere@ujf-grenoble.fr

*Contributed equally to this work.

Keywords
microtubule-targeting agents; azaindole; high-throughput screening; cell-based assay

Received
11 April 2012
Revised
20 July 2012
Accepted
10 August 2012

BACKGROUND AND PURPOSE

Drugs targeting microtubules are commonly used for cancer treatment. However, the potency of microtubule inhibitors used clinically is limited by the emergence of resistance. We thus designed a strategy to find new cell-permeable microtubule-targeting agents.

EXPERIMENTAL APPROACH

Using a cell-based assay designed to probe for microtubule polymerization status, we screened a chemical library and identified two azaindole derivatives, CM01 and CM02, as cell-permeable microtubule-depolymerizing agents. The mechanism of the anti-tumour effects of these two compounds was further investigated both *in vivo* and *in vitro*.

KEY RESULTS

CM01 and CM02 induced G2/M cell cycle arrest and exerted potent cytostatic effects on several cancer cell lines including multidrug-resistant (MDR) cell lines. *In vitro* experiments revealed that the azaindole derivatives inhibited tubulin polymerization and competed with colchicines for this effect, strongly indicating that tubulin is the cellular target of these azaindole derivatives. *In vivo* experiments, using a chicken chorioallantoic xenograft tumour assay, established that these compounds exert a potent anti-tumour effect. Furthermore, an assay probing the growth of vessels out of endothelial cell spheroids showed that CM01 and CM02 exert anti-angiogenic activities.

CONCLUSIONS AND IMPLICATIONS

CM01 and CM02 are reversible microtubule-depolymerizing agents that exert potent cytostatic effects on human cancer cells of diverse origins, including MDR cells. They were also shown to inhibit angiogenesis and tumour growth in chorioallantoic breast cancer xenografts. Hence, these azaindole derivatives are attractive candidates for further preclinical investigations.

Abbreviations

CM01, 4-chloro-2-(1-(4-methoxyphenyl)ethyl)-1-methyl-1H-pyrrolo[3,2-c]pyridine; CM02, 4-chloro-2-(1-(4-methoxyphenyl)vinyl)-1-methyl-1H-pyrrolo[3,2-c]pyridine; MDR, multidrug-resistant; SAR, structure–activity relationship

Introduction

Microtubules are dynamic structures composed of α-β-tubulin heterodimers that organize the cytoplasm during interphase and segregate condensed chromosomes during mitosis. They exhibit non-equilibrium dynamics, characterized by periods of polymerization and of depolymerization. These intrinsic microtubule dynamics are tightly regulated in the cell by interaction with an array of proteins that stabilize or destabilize microtubules, such as XMAP215/Dis1/TOGp, MCAK, MAP4 and Op18/stathmin (Holmfeldt *et al.*, 2009; Kavallaris, 2010) or +TIPs (plus-end tracking proteins) such as EB1 (Small and Kaverina, 2003; Akhmanova and Hoogenraad, 2005; Coquelle *et al.*, 2009). Targeted perturbation of this finely tuned process constitutes a major therapeutic strategy (Honore *et al.*, 2005). Anti-mitotic drugs that interfere with the microtubule system are, indeed, key components of combination chemotherapies for the treatment of carcinomas (Kavallaris, 2010).

Numerous compounds bind to the tubulin–microtubule system. They can be roughly classified into microtubule stabilizers (taxanes, epothilones, laulimalide, peloruside, discodermolide, dictyostatin, ABI-007, CT-2103, eleutherobin, sarcodictyins) and microtubule destabilizers (nocodazole, colchicine, combretastatin, vinca alkaloids, cryptophycin, eribulin, dolastatin, halichondrin, 2-methoxyestradiol, sulfonamide) (Calligaris *et al.*, 2010; Kavallaris, 2010).

However, the potency of microtubule inhibitors used clinically is limited by the emergence of resistance. This phenomenon is a multifactorial process (Kavallaris *et al.*, 1997; Kavallaris, 2010), but a common way for cancer cells to acquire drug resistance is the expression of efflux pumps such as the P-glycoprotein or *ABCG2* and *MRP1*. Thus, the identification of compounds that are active in multidrug-resistant (MDR) cells is urgently needed (Nien *et al.*, 2010).

High-throughput, cell-based screening of small molecules is an attractive strategy to identify such agents; it enables the evaluation of the activity of compounds directly on cells, ruling out molecules that are not cell-permeable or too toxic. In the past few years, several microtubule polymerization inhibitors such as 4-arylaminoquinazolines (Kasibhatla *et al.*, 2007) and micropolyin (De Rycker *et al.*, 2009) have been detected using cell-based assays.

We have set up a cell-based assay (Vassal *et al.*, 2006) that relies on the substrate properties of the tubulin-modifying enzymes involved in the tubulin tyrosination cycle (Lafanechere *et al.*, 1998; Lafanechere and Job, 2000; Peris *et al.*, 2006). This assay enables us to detect both microtubule-destabilizing and microtubule-stabilizing agents, in a single screening campaign (Lafanechere, 2008).

In the present work, using this innovative assay, we identified azaindole derivatives as microtubule polymerization inhibitors. Follow-up studies revealed that these compounds bind directly to tubulin and impede colchicine binding. Moreover, these azaindole derivatives induced G2/M cell cycle arrest and were toxic for a panel of cancer cell lines including MDR cell lines. These compounds also displayed potent anti-angiogenic properties and exerted an anti-cancer effect. The relevance of this class of molecules as new leads for drug development is discussed.

Methods

Chemicals

CM01, CM02 and all the other compounds studied were synthesized according to a method published previously (Nguyen *et al.*, 1986). The compound 3,4-dichloro CM07 was obtained by incubating $POCl_3$ in the presence of PCl_5 (1 equivalent, 56% yield). The following procedure was followed to obtain the compound 4-chloro-1-methyl-1*H*-pyrrolo[3,2-*c*]pyridin-2-yl)diphenylmethanol (CM08): a solution of ^{t}BuLi (1.6 N in heptane, 15.6 mL, 25 mmol) was added dropwise to a solution of 4-chloro-1-methyl-1*H*-pyrrolo[3,2-*c*]pyridine (3.33 g, 20 mmol) in anhydrous tetrahydrofuran (THF) (120 mL) at −65°C under nitrogen. The whole solution was stirred at the same temperature for 10 min. A solution of benzophenone (3.6 g, 20 mmol) in THF (20 mL) was then added dropwise and the resulting solution stirred at −20°C for 30 min, then at room temperature for 2 h. Then, 250 mL of 4 N HCl solution was added and the precipitate was collected by filtration after 18 h stirring at room temperature and washed with water. Following recrystallization from ethanol, the pure expected compound was obtained (5.6 g, 80% yield), mp 258°C. Elemental analysis $C_{21}H_{17}ClN_2O$; Calcd: C, 72.31; H, 4.91; Cl, 10.16; N, 8.03; Found: C, 72.24; H, 5.04; Cl, 9.98; N, 7.84.

Stock solutions (10 mM) were prepared in DMSO and kept at −20°C. Appropriate dilutions were freshly prepared just before use.

Paclitaxel, colchicine and vinblastine were purchased from Sigma-Aldrich (Saint Quentin-Fallavier, France). [^{3}H]-colchicine and [^{3}H]-vinblastine were obtained from NEN (Boston, MA, USA) and GE Healthcare (Velizy, France) respectively.

Screening. The screen was performed as described by Vassal *et al.* (2006). Briefly, HeLa cells were seeded, at a density of 36 000 cells per well, on 96-well polystyrene tissue culture plates in 90 µL of medium and were allowed to grow for 24 h. The following day, each well was robotically supplemented with 10 µL of RPMI containing compounds (6560) from the Centre National pour la Recherche Scientifique-Curie Institute library. The final concentration of the each compound was 25 µM. For bioactive controls, the final concentration was 5 µM for paclitaxel and 2 µM for colchicine. The final concentration of DMSO was 0.5%. After the compounds had been added, the cells were incubated for 2 h at 37°C, in 5% CO_2 in the the workstation incubator. Cells were then permeabilized, by addition of 100 µL of warm optimal (OPT) buffer for 10 min, in order to eliminate free, depolymerized tubulin, and fixed by addition of 100 µL of methanol for 6 min. Cells were then double stained for tyrosinated and detyrosinated tubulin using specific antibodies and fluorescent secondary antibodies. Nuclei were stained with Hoechst. Fluorescence was measured using the FLUOstar Optima microplate reader (BMG), with suitable filters for each wavelength. Raw data were converted into percentage of tyrosinated/detyrosinated tubulin contents, based on average results obtained from plate controls. Linear regression was measured based on plate control averages so as to reduce the impact of plate effects. Compounds shown to be active in this

primary screening method were retested from freshly made solutions.

Human mammary epithelial cells (HMEC)-GFP preparation. HMEC-1 cells were infected by a defective retrovirus encoding for EGFP. A DNA construct encoding both the EGFP coding sequence under the control of the herpetic human cytomegalovirus promoter and the neo gene (vector pEGFP-N1, Clontech, Mountain View, CA, USA) was cloned into the pLNCX vector. This vector was integrated into PT67 cells by transfection with Effectene (Qiagen, Valencia, CA, USA). PT67 cell supernatants were used to infect HMEC-1 cells. HMEC-1 clones expressing EGFP were selected in the presence of neomycin. Resistant clones were isolated by limit dilution, and amplified as independent lineages. One cell line strongly expressing EGFP protein was named HMEC-GFP.

Sprouting of HMEC-GFP. To prepare spheroids, HMEC-GFP cells were seeded at 3000 cells per well in round-bottom 96-multiwell plates in DMEM containing 1 $g \cdot L^{-1}$ glucose (Eurobio, Les Ulis, France) and 0.25% methylcellulose. Forty-eight hours later, the spheroids were collected, transferred into flat-bottom 96-well plates and embedded in collagen gel (1.2 $mg \cdot mL^{-1}$ type I collagen) prepared in an Iscove's modified Dulbecco's medium, supplemented with fibroblast growth factor 2 (FGF2) (10 $ng \cdot mL^{-1}$), 50 $U \cdot mL^{-1}$ penicillin and 50 $\mu g \cdot mL^{-1}$ streptomycin. Treatment with two concentrations (25 μM and 12.5 μM) of CM01 and CM02 was started immediately after the spheroids had been embedded in the collagen gels. Sprouting was allowed for 24 h at 37°C. Images were acquired by fluorescence microscopy and analysis of gel invasion was performed using the freeware ImageJ (http://rsbweb.nih.gov/ij/). Statistical analysis was performed using a Kruskal–Wallis test.

Chick embryo tumour growth and metastasis assay. MDA-MB-231 cells were transfected with GFP-encoding plasmid pEGFP-N1 (Clontech) using FuGENE® reagent (Roche, Indianapolis, IN, USA) and stable cells clones (MDA-MB-231-GFP) were selected. Fertilized White Leghorn eggs (SFPA, St. Brieuc) were incubated at 38°C with 60% relative humidity for 10 days. At this time (E10), the chorioallantoic membrane (CAM) was dropped by drilling a small hole through the eggshell into the air sac and a 1 cm^2 window was cut in the eggshell above the CAM.

Cultured MDA-MB-231-GFP were detached by trypsinization, washed with complete medium and suspended in serum-free DMEM. A 50 μL inoculum of 1 x 10^6 MDA-MB-231-GFP cells was added directly onto the CAM of each egg. Eggs were then randomly allocated into four groups of 12 eggs (to get enough surviving embryos at the end of the experiments). Two days later, tumours could be detected. They were then treated for 8 days, every two days (E12, E14, E16, E18), by dropping 100 μL of either 50 μM CM01, 50 μM CM02, 2 μM colchicine or 0.5% DMSO (vehicle) in PBS onto the tumour. The dropwise addition of a solution onto the large tumour area that depresses the CAM surface was found to be a suitable method, which avoided leakage and dispersion of the compounds. Then, the windows were sealed with cellophane tape and the eggs were returned to the incubator. At E19, the upper portion of the CAM was removed, transferred into PBS and the tumours were then carefully cut away from normal CAM tissue. Tumours were then quickly dried on cellophane before being weighed. In parallel, a 1 cm^2 portion of the lower CAM was collected to evaluate the number of nodules containing GFP-expressing cells. The fluorescent nodule were visualized *in situ* using whole mounts of tissue fixed in 4% formaldehyde in PBS and flattened between a hollow glass slide and a thick coverslip. A thorough and complete visual scan of a section of the lower CAM was performed using Leica Macrofluo fluorescent microscope (Optimal, Grenoble). Digital colour images were acquired using DP25 camera on SZX10 microscope (Olympus, France).

Other procedures are described in the Supporting Information Appendix S1.

Results

A cell-based screen identifies azaindole derivatives as reversible microtubule polymerization inhibitors

The assay used to screen the chemical library was based on the substrate properties of the tubulin-modifying enzymes involved in the tubulin tyrosination cycle. In this cycle, the C-terminal tyrosine of the tubulin α-subunit is removed by a carboxypeptidase and re-introduced by tubulin tyrosine ligase. Because of the substrate properties of these enzymes, dynamic microtubules, sensitive to depolymerizing drugs, are composed of tyrosinated tubulin, whereas non-dynamic, stabilized microtubules are composed of detyrosinated tubulin. Thus, depolymerization or stabilization of the microtubule network can be easily distinguished by double-immunofluorescence staining using antibodies specific for tyrosinated and detyrosinated tubulin. This assay was used to screen a library of 6560 compounds at a concentration of 25 μM. We selected 158 compounds belonging to several distinct structural families and able to lower the signal down to at least 75% in the tyrosinated tubulin channel as compared with DMSO-treated cells. The normal Hoechst signal observed with these compounds is an indirect estimation of the integrity of the cell monolayer. Hence, our results indicated that the compounds identified were potential microtubule-depolymerizing agents (Supporting Information Table S1). Among them, we first focused on two potent azaindole derivatives, CM01 and CM02, because their scaffolds were drug-like and simple and their synthesis could provide an easy access to numerous derivatives. Their effect on cellular microtubules was confirmed by immunofluorescence on HeLa cells fixed after permeabilization with OPT buffer. Whereas DMSO-treated cells exhibited a normal filamentous microtubule array, CM01/CM02-treated cells, similar to colchicine-treated cells, were devoid of microtubules (Figure 1A). We also checked for changes in tubulin polymerization status by performing sequential extraction of soluble and insoluble pools of cellular tubulin. This enables the separation of unpolymerized or depolymerized tubulin from microtubules. We tested decreasing concentrations (from 25 to 1 μM) of CM01 (Figure 1B) and CM02 (Figure 1C) and, whatever the concentration tested, we observed a shift towards the unpolymerized tubulin pool, similar to the effect elicited by colchicine. We then analysed in-depth the effects of CM01 and CM02 on

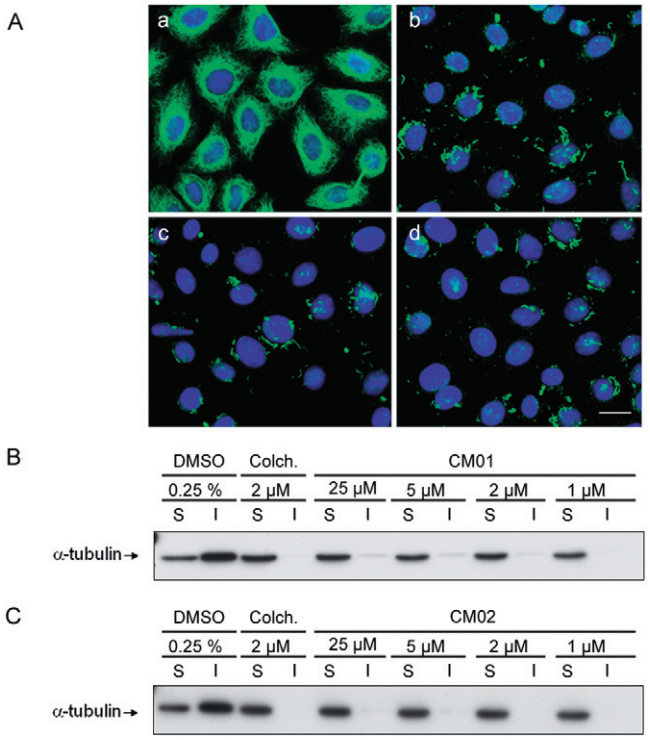

Figure 1

Effect of CM01 and CM02 on microtubule network organization. (A) Immunofluorescence analysis of cell microtubules. HeLa cells were incubated for 2 h with 0.25% DMSO (panel a, vehicle control), 5 μM colchicine (panel b), 25 μM CM01 (panel c) or 25 μM CM02 (panel d). Cells were then permeabilized, fixed and stained for tubulin (green) as described in Methods. Nuclei were stained with Hoechst (blue) Bar = 10 μm. (B) α-Tubulin partition between soluble and insoluble fractions. HeLa cells were treated for 2 h with 0.25% DMSO (vehicle control), 2 μM colchicine and increasing concentrations of CM01 as indicated. Insoluble (I) and soluble (S) fractions were prepared as described in Methods. Equivalent volumes of extracts (20 μL) were separated on 8% SDS-PAGE, and subjected to immunoblot analysis using monoclonal antibody specific for total α-tubulin. (C) same as (B), but with CM02.

microtubule dynamic instability parameters, using time-lapse fluorescence microscopy on GFP-EB3 transfected cells (Honore and Braguer, 2011) and compared them with those of colchicine. The concentrations assayed were determined after a preliminary immunofluorescence analysis of the compounds effect on the microtubule network. The concentrations chosen were in the range that induced a detectable but not total depolymerization of the microtubule network. Similar to colchicine, CM01 and CM02 reduced the microtubule growth rate, increased time spent in pause and strongly reduced the microtubule growth length, as indicated by the dose-dependent increase in the distance-based catastrophe frequency (Table 1). These results clearly show that CM01 and CM02 have a strong effect on microtubule dynamics.

We also tested whether the microtubule-depolymerizing effect induced by CM01 and CM02 is reversible (Supporting Information Figure S1), by replacing medium containing the compounds with standard culture medium. Immunostaining of α-tubulin revealed that after removal of the test compounds normal microtubule array was restored. These results demonstrate that CM01 and CM02 are cell-permeable reversible microtubule polymerization inhibitors.

Azaindole derivatives are tubulin binders and compete with colchicine

To determine whether tubulin was the target site of azaindole derivatives, *in vitro* microtubule polymerization assays were performed using either microtubule protein or pure tubulin (Figure 2A). In both cases, CM01 and CM02 inhibited tubulin polymerization in a dose-dependent manner. To determine the binding site of the compounds on tubulin, the effects of CM01 and CM02 on the tubulin binding of [^{3}H]-colchicine and [^{3}H]-vinblastine were investigated (Figure 2B). CM01 and CM02 selectively inhibited colchicine but not vinblastine binding on tubulin. These results indicate that tubulin is a target of azaindole derivatives and that azaindole derivatives bind to the colchicine-binding site but not to the vincaalkaloids site.

Structure–activity relationships (SAR) analysis

To explore the chemical properties conferring inhibitory potency to azaindole derivatives, we selected and tested several analogues of this family of compounds (Table 2). These assays were first conducted on *in vitro* tubulin assembly. The effects of the compounds were compared at a concentration of 25 μM. We first investigated the requirements of the inter-aromatic group Z. The inhibitory potencies of the compounds were the same when an ethane (CM01), an ethylene (CM02) or a hydroxyethyl (CM05) was present in this position, which indicates that the nature of group Z is not a stringent determinant of inhibitory potency. Position R1 can also be substituted by either a small group (methyl, CM01 and CM02) or by a larger one (benzyl, CM03 and CM04) without loss of inhibitory potency, which indicates some tolerance to bulky substituents at position R1. Substitution of hydrogen by a chlorine group at position R2 (CM07) did not alter the inhibitory potency of the compound. In contrast, the presence of a methoxy group at position R3 was a crucial requirement for the compound to be active, as illustrated by the results obtained with CM06 and CM08. We next investigated whether the *in vitro* SAR correlated with cellular effect on microtubule network upon treatment with azaindole derivatives. Cells grown on microplates were incubated with the different compounds, fixed and processed for immunofluorescence. The quantification was performed using the microplate reader, in the same way as for the primary screening. A good correlation was observed, which supports that tubulin is indeed the cellular target of azaindole derivatives, responsible for the observed phenotype.

Azaindole derivatives inhibit cell proliferation of diverse cancer cell lines by promoting G2/M cell cycle arrest

Viability of carcinoma cell lines from several organs (cervix, kidney, lung and breast) in response to CM01 and CM02 treatment was investigated using MTT assays (Table 3). GI_{50} (50% of growth inhibition) values were in the sub- or low-micromolar range regardless of the tissue origins, p53 or K-*ras* status of the cells. To determine the mode of action of the

Table 1

Comparison of alteration of microtubule dynamic instability parameters induced by colchicine with that of CM01 and CM02

Parameters	DMSO	Colchicine 0.05 μM	Colchicine 0.1 μM
% time spent growing	77.69	73.44	64.99
% time spent in pause	22.31	26.56	35.01
Growing rate (μm·min^{-1})	17.04 ± 0.22	15.32 ± 0.37***	14.66 ± 0.28***
Catastrophe frequency (μm^{-1})	0.21 ± 0.01	0.33 ± 0.04**	0.40 ± 0.04***
Catastrophe frequency (min^{-1})	2.83 ± 0.08	3.56 ± 0.29*	3.71 ± 0.35*

Parameters	CM01 0.05 μM	CM01 0.1 μM	CM02 0.05 μM	CM02 0.1 μM
% time spent growing	59.70	49.86	55.77	42.64
% time spent in pause	40.30	50.14	44.23	57.36
Growing rate (μm·min^{-1})	14.04 ± 0.36***	13.18 ± 0.30***	13.35 ± 0.38***	12.43 ± 0.31***
Catastrophe frequency (μm^{-1})	0.34 ± 0.03***	0.53 ± 0.04***	0.39 ± 0.03***	0.78 ± 0.08***
Catastrophe frequency (min^{-1})	2.68 ± 0.13	3.28 ± 0.18*	2.89 ± 0.20	3.87 ± 0.29**

If not %, data are presented as mean ± SEM. *P < 0.05; **P < 0.01, ***P < 0.001 significantly different from control values (DMSO) using Student's t-test.

anti-proliferative activity exhibited by azaindole derivatives, we used flow cytometry to analyse the distribution of CM01/CM02-treated cells in the cell cycle. Following a 16 h exposure of cells to the compounds at 1 μM or 25 μM, the percentage of cells accumulated in G2/M phases (>89%) were compared to that of vehicle-treated cells (23%, Figure 3).

Taken together, these results show that azaindole derivatives are potent cytostatic compounds, which block the cell cycle at the G2/M phase.

Azaindole derivatives overcome the drug-resistant (MDR) cell phenotype

We compared the effects of CM01 and CM02 on cell proliferation of drug-sensitive cell-lines with those of their drug-resistant counterparts that over-express the P-glycoprotein or multidrug transporters, such as *ABCG2* and *MRP1* that confer cell resistance to many drugs (Harker and Sikic, 1985) (Table 3). The toxic effects of CM01 and CM02 were found to be the same, with GI_{50} values in the μM range, for the drug-sensitive human cell lines, and for their MDR counterparts, indicating that these compounds are not substrates of P-glycoprotein or of *ABCG2* and *MRP1* transporters. This contrasts with the active efflux, at nM concentrations, of colchicine and taxanes (paclitaxel and docetaxel) by P-glycoprotein, and of vinca alkaloids (vincristine and vinblastine) by both P-glycoprotein and MRP1 (Dumontet *et al.*, 1996; Szakacs *et al.*, 2006; Fojo and Menefee, 2007).

Azaindole derivatives exhibit an anti-angiogenic effect

Numerous compounds, such as combretastatins, which bind to the tubulin colchicine-binding site, exhibit anti-angiogenic effects. To investigate the putative anti-angiogenic potency of azaindole derivatives, we tested CM01 and CM02 in two different *in vitro* angiogenesis assays. Firstly, we investigated the effect of the compounds on capillary-like tube formation on Matrigel and found that both compounds were able to inhibit capillary tubes morphogenesis (Figure 4). Secondly, we used a more integrated assay, that is three-dimensional cultures of HMEC-GFP cell spheroids in a collagen gel, and analysed the effects of increasing doses of the compounds on FGF2-stimulated endothelial cell sprouting. Although the compounds show no detectable toxicity on spheroids themselves (Figure 5A), they induced a dose-dependent decrease in the mean length of the total number of endothelial sprouts (Figure 5B). In both assays, CM02 showed a stronger effect than CM01. These data indicate that azaindole derivatives are potent anti-angiogenic compounds.

Azaindole derivatives exhibit an anti-tumour effect on an in vivo *model of invasive breast cancer*

We used breast cancer cells (MDA-MB-231 expressing GFP) xenografted on the chicken CAM to assess both the toxicity and efficacy of CM01 and CM02 molecules. Tumours treated with these compounds were significantly smaller (P < 0.05; Figure 6A and B).

Furthermore, treatment with CN01 and CM02 did not significantly increase the mortality of chicken embryos indicating that, in this model, these compounds are well tolerated at doses sufficient to induce an anti-tumour effect.

The expression of GFP by the highly invasive MDA-MB-231 cells allowed an accurate detection, using fluorescence microscopy, of the dissemination of tumour cells in this model, as indicated by the number of nodules counted in the lower CAM (Figure 6C) in DMSO-treated embryos. The

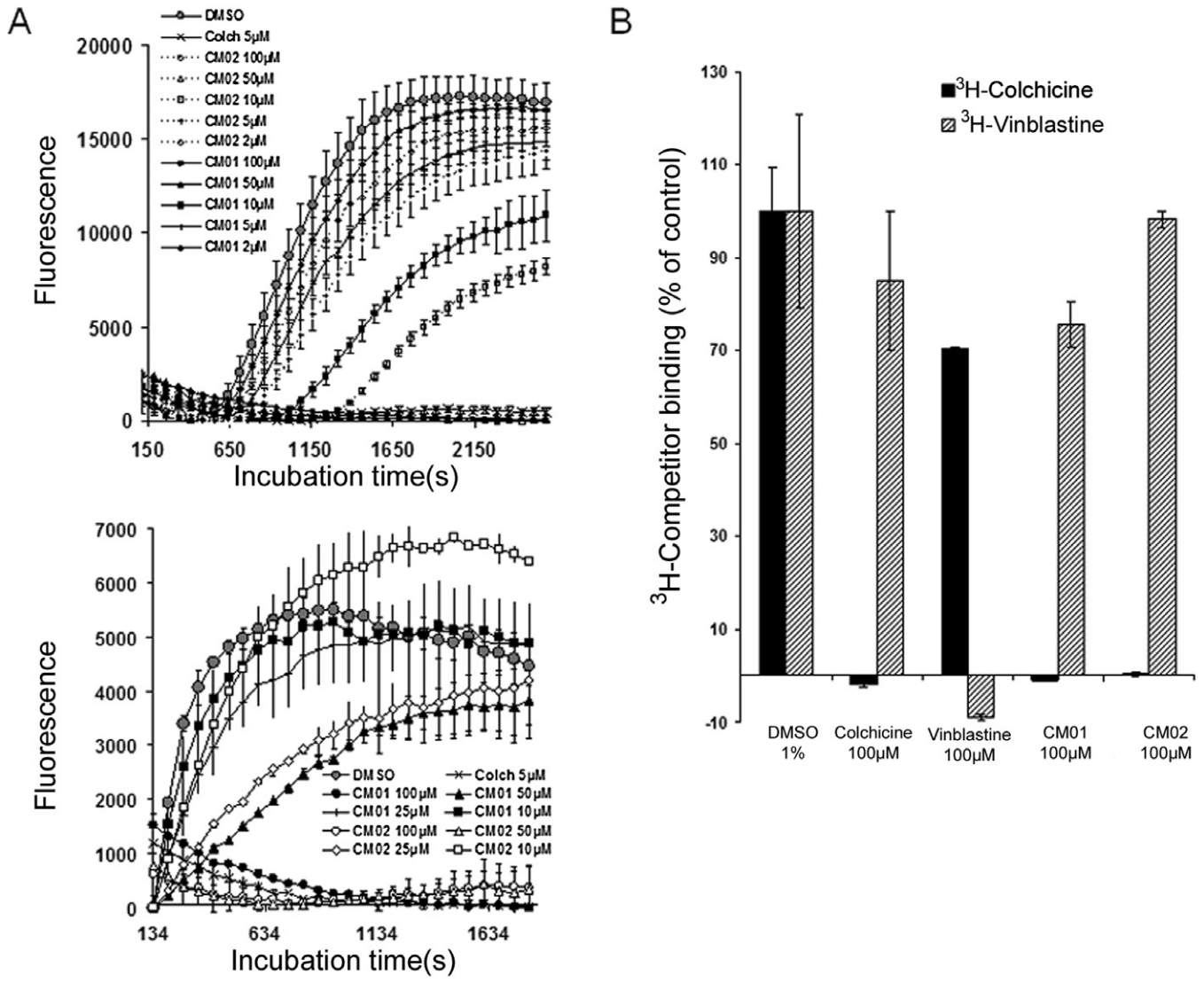

Figure 2

Effect of CM01 and CM02 on microtubule polymerization *in vitro*. (A) Microtubule protein (MTP) (upper graph) and pure tubulin (lower graph) polymerization assay. Tubulin was allowed to polymerize at 37°C, at the indicated conditions. Fluorescence of DAPI bound to microtubules was measured to monitor microtubule polymerization. Experiments were performed in triplicate, in the presence of increasing concentrations of CM01 or CM02, as indicated. Results are presented as mean ± SEM. (B) Effect of CM01 and CM02 on the binding of [^{3}H]-colchicine and [^{3}H]-vinblastine to MTPs. [^{3}H]-colchicine 50 nM or [^{3}H]-vinblastine 30 nM were used to competed with 100 µM CM01, CM02, colchicine and vinblastine as described in Methods. Each value represents the mean ± SEM from triplicate determinations.

nodule number was greatly reduced in CM01- and CM02-treated embryos, indicating that azaindole derivatives inhibit tumour growth by affecting invasion mechanisms.

Discussion

Regulation of microtubule dynamics is crucial for complex biological processes such as cell cycle, shape maintenance or motility. Moreover, the microtubule system is a key component of the mitotic apparatus. Perturbation of microtubule dynamics by drugs constitutes one of the most powerful ways to suppress (at least transiently) tumour growth. Microtubule-binding drugs generally achieve a clinical response by stalling cell cycle at G2/M phase as a result of abnormal mitotic spindle assembly and chromosome segregation (Kavallaris, 2010). Despite their massive clinical use, the therapeutic potential of most of these drugs is hampered by insufficient bioavailability and toxicity (myelosuppression, peripheral neurotoxicity). Moreover, failure in cancer therapy is often associated with tumour cells that have acquired resistance to microtubule-binding drugs. As a result, much effort has been invested to identify new chemical entities that can be used to overcome these resistance

Table 2

In vitro and cellular tubulin polymerization inhibitory activities of azaindole derivatives

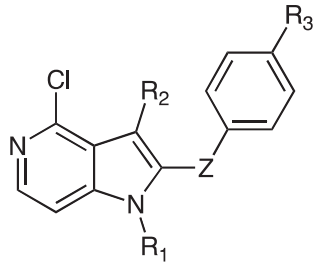

Compound	Substituents at position RI	R2	R3	Z	Tubulin assembly (%)	Tyr-Tubulin signal (%)
CM01	CH_3	H	OCH_3	$CH(CH_3)$	0.0	0.0
CM02	CH_3	H	OCH_3	$C = CH_2$	0.0	0.0
CM03	Bn	H	OCH_3	$CH(CH_3)$	11.5	27.6
CM04	Bn	H	OCH_3	C = CH2	3.8	30.9
CM05	CH_3	H	OCH_3	$C(OH)CH_3$	0.9	10.0
CM06	CH_3	H	H	$CH(CH_3)$	66.7	101.3
CM07	CH_3	Cl	OCH_3	$CH(CH_3)$	9.6	0.0
CM08	CH_3	H	H	C(OH)Ph	100.2	82.6

The effects of the derivatives (25 μM) were analysed on *in vitro* microtubule protein polymerization assays and using quantitative tubulin immunostaining of HeLa cells. In this later experiment, cells grown in microplates were incubated for 2 h with the different compounds or with DMSO, fixed and processed for immunofluorescence. The quantification was performed using the microplate reader. Results are expressed as percentage of the signal obtained on DMSO-treated samples (100%).

Table 3

Effects of azaindole derivatives on the viability of different cell lines

Cell line	Type	Concentration of CM01 that inhibits 50% of the cell growth	Concentration of CM02 that inhibits 50% of the cell growth
HeLa	Human cervical adenocarcinoma	0.5 μM	0.7 μM
786-O	Human renal adenocarcinoma	0.4 μM	1.3 μM
NCI H460	Human lung carcinoma	0.3 μM	1.0 μM
MCF-7	Human breast adenocarcinoma	1.2 μM	12.7 μM
MDA-MB-231	Human breast carcinoma	0.1 μM	0.2 μM
MES-SA	Human uterine sarcoma	0.3 μM	1.0 μM
MES-SA/DX5	Multidrug-resistant cell line derived from the MES-SA	0.3 μM	0.7 μM
HEK-293	Cell line derived from human embryonic kidney	0.3 μM	0.1 μM
HEK-293-ABCG2	HEK-293 stably transfected with the *ABCG2* transporter	0.4 μM	0.4 μM
BHK-21	Cell line derived from baby hamster kidney	0.1 μM	0.1 μM
BHK-21-MRP1	BHK-21 stably transfected with *MRP1* (multidrug resistance protein 1)	0.1 μM	0.1 μM

Cells were treated with various concentrations of compounds for 48 h and their viability was evaluated using MTT metabolic assay. The GI_{50} (concentration giving 50% inhibition of cell growth) values were calculated from the log dose–response curve and are presented in μM. The values represent the means of three independent determinations.

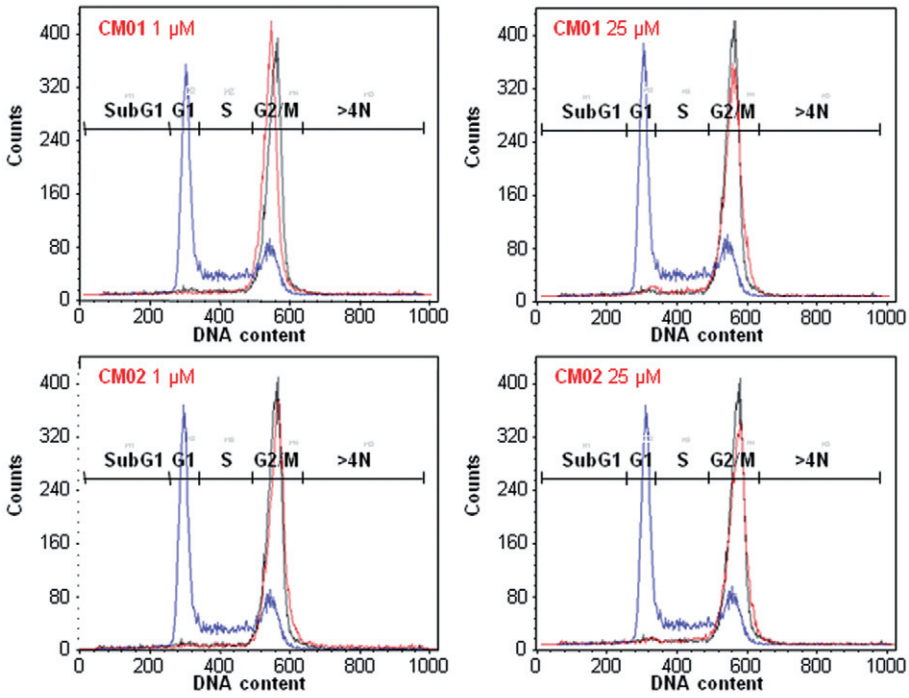

	SubG1	G1	S	G2/M	>4N
DMSO	1.25	55.01	20.33	22.98	0.43
Colchicine 2 µM	1.88	2.27	3.56	90.71	1.59
CM01 1 µM	1.12	1.07	3.66	91.45	2.70
CM01 25 µM	1.22	3.04	4.89	89.01	1.84
CM02 1 µM	1.22	1.39	2.89	89.79	4.71
CM02 25 µM	1.39	2.12	4.80	89.71	1.98

Figure 3

Cell cycle distribution after treatment of HeLa cells with CM01 or CM02. HeLa cells were incubated for 16 h with DMSO (control), colchicine (2 µM), CM01 or CM02 (1 µM and 25 µM, as indicated). Cell cycle parameters were analysed by flow cytometry, as described in Methods. The upper panel shows the graphs obtained for 1 and 25 µM, as indicated, of CM01 and CM02 (red), compared with that obtained for DMSO (blue). Values (lower table) are expressed as percentage of the total cell population.

mechanisms [5-amino-2-aroylquinolines (Nien *et al.*, 2010), 1,2,4-triazole (Arora *et al.*, 2009)].

In the present study, using a cell-based assay, we identified a new class of azaindole derivatives as compounds that disrupt microtubule array in a reversible manner. Reversibility probably rules out the possibility of covalent bond formation between tubulin and azaindole derivatives. Since reversibility generally enables better control of the dose administered during treatment, this characteristic is of importance for lead development. Biochemical experiments indicated that tubulin is an *in vitro* target of azaindole derivatives and its polymerization inhibition is likely responsible for the observed phenotype. However, complete microtubule depolymerization was observed in cells, at lower concentrations (0.05 to 1 µM) than those needed for complete depolymerization of just microtubules *in vitro*. This difference could be explained by the fact that true intracellular concentrations of the compounds are not really known and result not only from equilibrium between uptake and efflux of the compounds, but also from affinity with their target.

Competition assays using tritiated colchicine and vinblastine indicated that azaindole derivatives bind tubulin directly at a site that, at least partially, overlaps the colchicine site. However, from our experiments, we cannot exclude the possibility that azaindole derivatives inhibit colchicine binding by an allosteric mechanism. The toxicity induced by colchicine treatment hampers its use as an anti-cancer drug. Currently, there are no colchicine-binding site drugs approved by the Food and Drug Administration for the treatment of cancer. Combretastatins and sulfonamides that bind to the same site are, however, presently undergoing Phase I and II clinical trials for solid tumours (Nien *et al.*, 2010). This confirms the druggability of this particular binding site and further confirms that azaindole derivatives are suitable lead conpounds for drug optimization programmes. By testing several analogues we identified essential features for tubulin binding and activity in cell. Since SAR established using a cell-based assay may be biased by the cellular permeability and stability of the tested compounds, we conducted an in parallel SAR analysis of the compounds' effects on tubulin

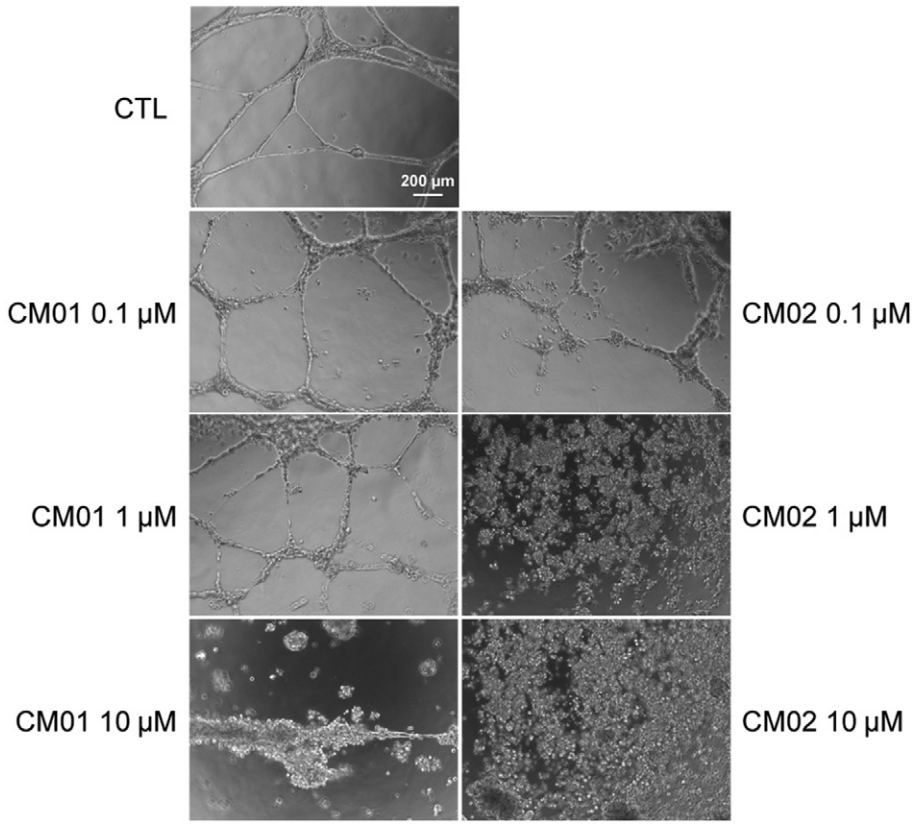

Figure 4

Azaindole derivatives inhibit capillary-like tube formation. HUVEC cells were seeded on Matrigel and compounds at the indicated concentrations were added after cell attachment (one hour later). Tubule formation was observed by phase-contrast microscopy at 24 h. Bar = 200 µm.

in vitro polymerization. These analyses gave similar results and indicated that positions R1, R2 and inter-aromatic group Z are tolerant to substitution, whereas a methoxy group in position R3 is required for the compound to be active. This is in agreement with results from a previous study in which the methoxy group was identified as a crucial feature for colchicine and related compounds to be active (Nguyen *et al.*, 2005). Moreover, the observation that the *in vitro* SAR closely parallels the effects observed on cellular microtubule network supports the assumption that tubulin is the cellular target of azaindole derivatives.

The antiproliferative activities of the azaindole derivatives revealed a broad spectrum of cytostatic effect with comparable efficacies on cell lines that were deficient in p53 or overexpressed K-*ras*, both genetic and epigenetic alterations that are among the most common alterations found in cancer cells. In addition, in contrast to many clinically-used microtubule-binding drugs, the azaindole derivatives also exhibited anti-proliferative activity in cell lines overexpressing the drug efflux pumps PgP, MRP1 and ABCG2. As the action of azaindole derivatives is reversible, these compounds may thus be used as a research tool for cell synchronization experiments with resistant cells. Moreover, this property could be exploited in cases of chemotherapeutic failure.

Flow cytometry analysis revealed that azaindole derivatives exert their anti-proliferative action through cell cycle arrest at the G2/M phase. Aneuploid cells were detected following treatment with azaindole derivatives. The induction of aneuploidy could be a concern since it promotes genetic instability. However, most if not all microtubule-targeting compounds (for instance, vincaalkaloids) induce aneuploidy but remain valuable drugs.

Targeting tumour angiogenesis has become a major focus of anti-cancer research. Microtubule-targeting compounds have received considerable interest as potential anti-angiogenic and vascular-disrupting agents (Pasquier *et al.*, 2005; Jordan and Kamath, 2007). Although this effect could be attributed to a general cell toxic effect of microtubule poisons, some of the vascular-targeting agents that are now under development seem to damage the tumour vasculature without significantly harming normal tissue (Prise *et al.*, 2002). The basis of this specificity is not known. One possibility is that the intracellular levels of microtubule-targeting agents accumulating in endothelial cells is approximately five times higher than other cells (Vacca *et al.*, 1999; Merchan *et al.*, 2005), and this can, at least partly, account for the specific targeting of tumour vessels. Another possibility is that, since the tumour neovessels are highly proliferative compared to the quiescent endothelium of the host body, this vascular compartment of the tumours is also more susceptible to anti-microtubule agents, especially when low-dose metronomic delivery protocols are used (Gasparini, 2001). Moreover, for microtubule-targeting compounds such as vin-

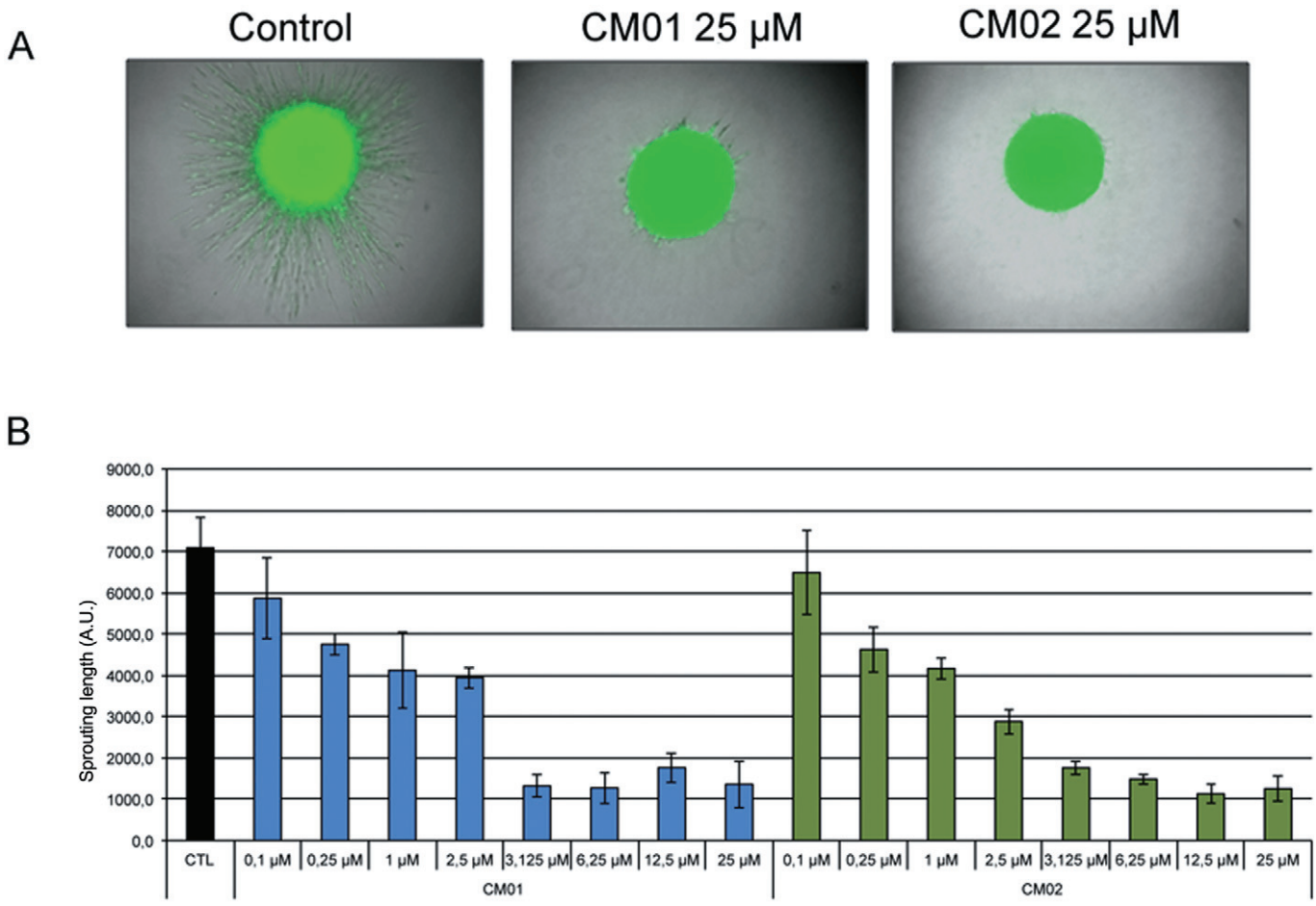

Figure 5

Quantitative analysis of endothelial sprouting in response to azaindole derivatives. FGF2 (100 ng·mL^{-1}) was added at day 0 to collagen-embedded HMEC-GFP spheroids in the presence of CM01 or CM02 at different concentrations (0.1 µM to 25 µM). After 3 days of culture, the spheroids were observed under an epifluorescence microscope. (A) Overlay of phase contrast and fluorescence observations at the indicated concentrations of compounds. (B) Measure of the mean total sprout length of endothelial spheroids, performed by quantitative microscopy image analysis. In each condition, data represent the mean values ± SEM of multiple spheroids (n > 10) from one representative experiment out of two.

flunin, it has been shown that non-cytotoxic concentrations inhibit capillary-like tube formation with a concomitant increase in interphase microtubule dynamic instability, which highlights the crucial role of interphase microtubule dynamics in angiogenesis (Pourroy *et al.*, 2006; Honore *et al.*, 2008).

It has also been suggested that this specific targeting of tumour cells could be due to differences between the mature vasculature of normal tissues and the immature or forming vasculature of tumours (Tozer *et al.*, 2001). Such immature vessels show an increased permeability to macromolecules upon exposure to microtubule poisons. This protein leakage would lead to oedema and might cause a rapid increase in interstitial fluid pressure, leading to vascular collapse (Tozer *et al.*, 2005). Indeed, a mechanistic link between disruption of the microtubule cytoskeleton and inhibition of tumour angiogenesis via the hypoxia-inducible factor-1 pathway has been identified (Escuin *et al.*, 2005).

Our finding that azaindole derivatives inhibit angiogenic sprouting from microvascular endothelial cell spheroids strongly suggests that these compounds have the capacity to exert anti-angiogenic activity on tumour cells *in vivo*.

The standard assays normally used for evaluating the performance of anti-cancer drugs involve human tumour xenografts in immunodeficient mice. However, tumours grown on the CAM of embryonated chicken eggs constitute a fast, easy and affordable system for an initial preclinical analysis of the effects of a compound. The highly vascularized nature of the CAM greatly promotes the efficiency of tumour cell grafting. Remarkably, within 8 days, not only do MDA-MB-231 tumour cells develop sizable tumours, but also they can escape the primary site, invade surrounding stroma and reach distal portions of the CAM to form micro-metastasis foci. Therefore, similar to some murine models, all steps of tumour growth and of the metastatic cascade are replicated in the chick embryo model but, importantly, in a very short period of time.

We found that CM01 and CM02 administration, at a concentration that does not affect the embryos' development, significantly reduced the tumour size, as compared to

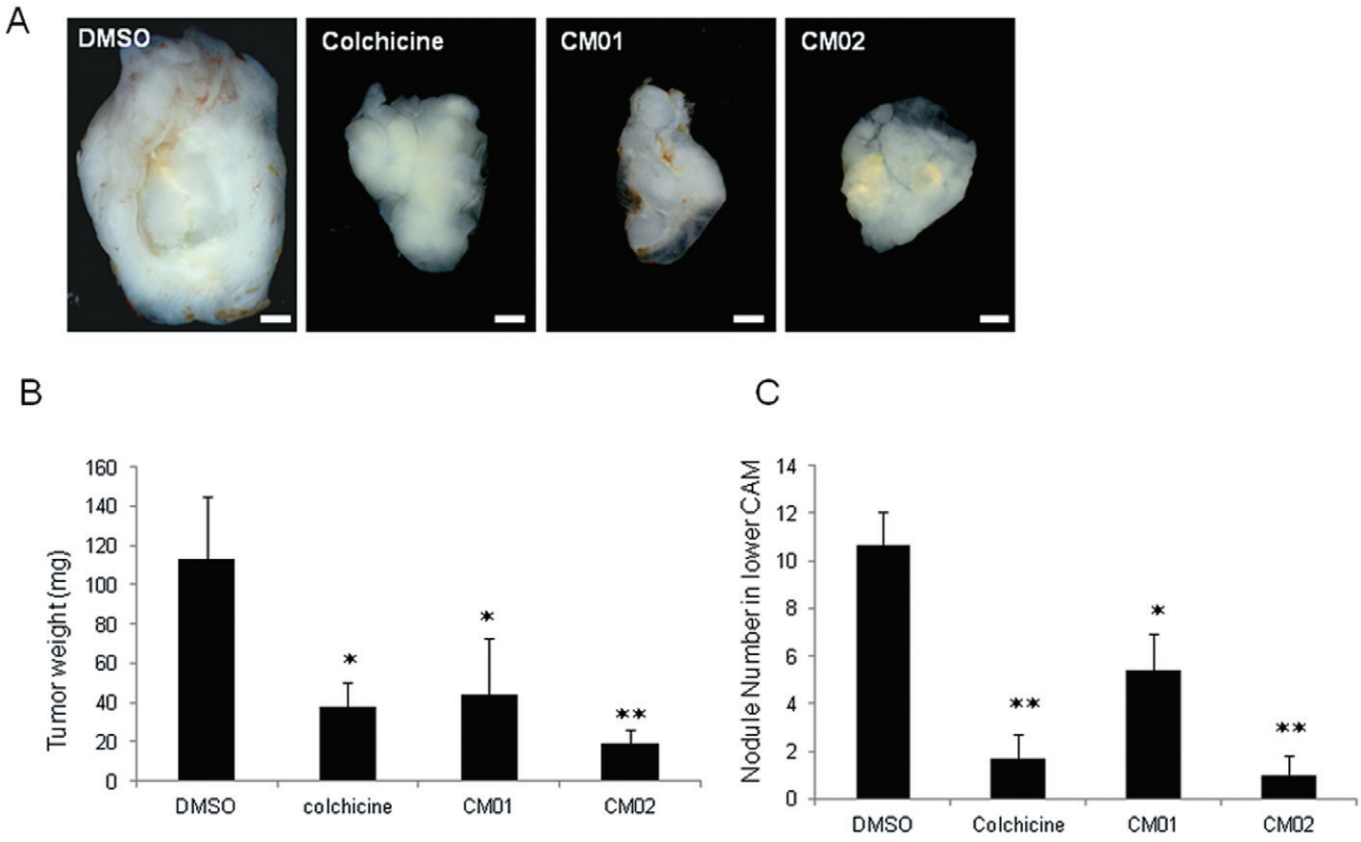

Figure 6

Anti-tumour effect of azaindole derivatives. MDA-MB-231 cells were xenografted on chick embryo chorioallantoic membrane (CAM). After treatment with either vehicle (DMSO), colchicine, CM01 or CM02, tumours were excised and weighed. The lower CAM was also dissected and fixed and the number of GFP-fluorescent nodules was counted, as described in the Methods section. (A) Representative pictures of tumours at the end of the different treatments. (B) Effect of the different treatments on tumour weight (means ± SEM of six samples). (C) Effect of the different treatments on the nodule number detected in the lower CAM (means ± SEM of six samples). *$P < 0.05$; **$P < 0.01$, significantly different from control values using Mann–Whitney test. Bar = 0.8 mm.

the vehicle (DMSO)-treated tumours. Furthermore, by comparing the number of nodules present in the lower CAM of CM01- and CM02-treated embryos with those of vehicle-treated embryos, we found that both compounds have anti-metastatic properties.

Azaindoles represent a huge family of chemical compounds, several of which have been found to have anti-cancer and anti-angiogenic properties, although through distinct mechanisms of action (Echalier *et al.*, 2008; Hong *et al.*, 2012). The azaindole derivatives described in the present study represent a novel class. They are reversible microtubule-depolymerizing agents that exert potent cytostatic effects on human cancer cells of diverse origins, including MDR cells. Although they act in the micromolar range, their chemical structure is simpler than those of microtubule polymerization inhibitors in current use. These molecules thus provide a useful platform for compound optimization. They were also shown to significantly inhibit angiogenesis and tumour growth in chorioallantoic breast cancer xenografts. Taken together, the present findings indicate that these azaindole derivatives are attractive candidates for further preclinical investigations.

Acknowledgements

This work was supported by the Centre National pour la Recherche Scientifique, the Commissariat à l'Energie atomique, the Institut Curie, the Alliance des Recherches sur le Cancer (an initiative of the Association pour la Recherche sur le Cancer) and Rhône-Alpes Region. R. P. is the recipient of a fellowship from Fondation de France. E. V.-S. was the recipient of a fellowship from Rhone-Alpes Region. Thanks also to the ChemAxon company (http://www.chemaxon.com) which has allowed the academic *TAMIS* software team (especially S. Wieczorek, S. Aci, C. Charavay and S. Roy) to freely use the *MarvinView* package, a helpful Graphic User Interface for viewing structure files and query results.

Conflict of interest

I declare no conflict of interest on behalf of all the authors.

References

Akhmanova A, Hoogenraad CC (2005). Microtubule plus-end-tracking proteins: mechanisms and functions. Curr Opin Cell Biol 17: 47–54.

Arora S, Wang XI, Keenan SM, Andaya C, Zhang Q, Peng Y *et al.* (2009). Novel microtubule polymerization inhibitor with potent antiproliferative and antitumor activity. Cancer Res 69: 1910–1915.

Calligaris D, Verdier-Pinard P, Devred F, Villard C, Braguer D, Lafitte D (2010). Microtubule targeting agents: from biophysics to proteomics. Cell Mol Life Sci 67: 1089–1104.

Coquelle FM, Vitre B, Arnal I (2009). Structural basis of EB1 effects on microtubule dynamics. Biochem Soc Trans 37 (Pt 5): 997–1001.

De Rycker M, Rigoreau L, Dowding S, Parker PJ (2009). A high-content, cell-based screen identifies micropolyin, a new inhibitor of microtubule dynamics. Chem Biol Drug Des 73: 599–610.

Dumontet C, Duran GE, Steger KA, Beketic-Oreskovic L, Sikic BI (1996). Resistance mechanisms in human sarcoma mutants derived by single-step exposure to paclitaxel (Taxol). Cancer Res 56: 1091–1097.

Echalier A, Bettayeb K, Ferandin Y, Lozach O, Clement M, Valette A *et al.* (2008). Meriolins (3-(pyrimidin-4-yl)-7-azaindoles): synthesis, kinase inhibitory activity, cellular effects, and structure of a CDK2/cyclin A/meriolin complex. J Med Chem 51: 737–751.

Escuin D, Kline ER, Giannakakou P (2005). Both microtubule-stabilizing and microtubule-destabilizing drugs inhibit hypoxia-inducible factor-1alpha accumulation and activity by disrupting microtubule function. Cancer Res 65: 9021–9028.

Fojo T, Menefee M (2007). Mechanisms of multidrug resistance: the potential role of microtubule-stabilizing agents. Ann Oncol 18 (Suppl. 5): v3–v8.

Gasparini G (2001). Metronomic scheduling: the future of chemotherapy? Lancet Oncol 2: 733–740.

Harker WG, Sikic BI (1985). Multidrug (pleiotropic) resistance in doxorubicin-selected variants of the human sarcoma cell line MES-SA. Cancer Res 45: 4091–4096.

Holmfeldt P, Sellin ME, Gullberg M (2009). Predominant regulators of tubulin monomer-polymer partitioning and their implication for cell polarization. Cell Mol Life Sci 66: 3263–3276.

Hong S, Kim J, Seo JH, Jung KH, Hong SS (2012). Design, synthesis, and evaluation of 3,5-disubstituted 7-azaindoles as trk inhibitors with anticancer and antiangiogenic activities. J Med Chem 55: 5337–5349.

Honore S, Braguer D (2011). Investigating microtubule dynamic instability using microtubule-targeting agents. Methods Mol Biol 777: 245–260.

Honore S, Pasquier E, Braguer D (2005). Understanding microtubule dynamics for improved cancer therapy. Cell Mol Life Sci 62: 3039–3056.

Honore S, Pagano A, Gauthier G, Bourgarel-Rey V, Verdier-Pinard P, Civiletti K *et al.* (2008). Antiangiogenic vinflunine affects EB1 localization and microtubule targeting to adhesion sites. Mol Cancer Ther 7: 2080–2089.

Jordan MA, Kamath K (2007). How do microtubule-targeted drugs work? An overview. Curr Cancer Drug Targets 7: 730–742.

Kasibhatla S, Baichwal V, Cai SX, Roth B, Skvortsova I, Skvortsov S *et al.* (2007). MPC-6827: a small-molecule inhibitor of microtubule formation that is not a substrate for multidrug resistance pumps. Cancer Res 67: 5865–5871.

Kavallaris M (2010). Microtubules and resistance to tubulin-binding agents. Nat Rev Cancer 10: 194–204.

Kavallaris M, Kuo DY, Burkhart CA, Regl DL, Norris MD, Haber M *et al.* (1997). Taxol-resistant epithelial ovarian tumors are associated with altered expression of specific beta-tubulin isotypes. J Clin Invest 100: 1282–1293.

Lafanechere L (2008). Chemogenomics and cancer chemotherapy: cell-based assays to screen for small molecules that impair microtubule dynamics. Comb Chem High Throughput Screen 11: 617–623.

Lafanechere L, Job D (2000). The third tubulin pool. Neurochem Res 25: 11–18.

Lafanechere L, Courtay-Cahen C, Kawakami T, Jacrot M, Rudiger M, Wehland J *et al.* (1998). Suppression of tubulin tyrosine ligase during tumor growth. J Cell Sci 111 (Pt 2): 171–181.

Merchan JR, Jayaram DR, Supko JG, He X, Bubley GJ, Sukhatme VP (2005). Increased endothelial uptake of paclitaxel as a potential mechanism for its antiangiogenic effects: potentiation by Cox-2 inhibition. Int J Cancer 113: 490–498.

Nguyen CH, Bisagni E, Lhoste JM (1986). Synthèse des dérivés N-5 substitués des 5H-pyrido [4,3-b] benzo [f] indoles, isomères des 6H-pyrido [4,3-b] carbazoles (ellipticines). Can J Chem 64: 454–551.

Nguyen TL, McGrath C, Hermone AR, Burnett JC, Zaharevitz DW, Day BW *et al.* (2005). A common pharmacophore for a diverse set of colchicine site inhibitors using a structure-based approach. J Med Chem 48: 6107–6116.

Nien CY, Chen YC, Kuo CC, Hsieh HP, Chang CY, Wu JS *et al.* (2010). 5-Amino-2-aroylquinolines as highly potent tubulin polymerization inhibitors. J Med Chem 53: 2309–2313.

Pasquier E, Honore S, Pourroy B, Jordan MA, Lehmann M, Briand C *et al.* (2005). Antiangiogenic concentrations of paclitaxel induce an increase in microtubule dynamics in endothelial cells but not in cancer cells. Cancer Res 65: 2433–2440.

Peris L, Thery M, Faure J, Saoudi Y, Lafanechere L, Chilton JK *et al.* (2006). Tubulin tyrosination is a major factor affecting the recruitment of CAP-Gly proteins at microtubule plus ends. J Cell Biol 174: 839–849.

Pourroy B, Honore S, Pasquier E, Bourgarel-Rey V, Kruczynski A, Briand C *et al.* (2006). Antiangiogenic concentrations of vinflunine increase the interphase microtubule dynamics and decrease the motility of endothelial cells. Cancer Res 66: 3256–3263.

Prise VE, Honess DJ, Stratford MR, Wilson J, Tozer GM (2002). The vascular response of tumor and normal tissues in the rat to the vascular targeting agent, combretastatin A-4-phosphate, at clinically relevant doses. Int J Oncol 21: 717–726.

Small JV, Kaverina I (2003). Microtubules meet substrate adhesions to arrange cell polarity. Curr Opin Cell Biol 15: 40–47.

Szakacs G, Paterson JK, Ludwig JA, Booth-Genthe C, Gottesman MM (2006). Targeting multidrug resistance in cancer. Nat Rev Drug Discov 5: 219–234.

Tozer GM, Prise VE, Wilson J, Cemazar M, Shan S, Dewhirst MW *et al.* (2001). Mechanisms associated with tumor vascular shut-down induced by combretastatin A-4 phosphate: intravital microscopy and measurement of vascular permeability. Cancer Res 61: 6413–6422.

Tozer GM, Kanthou C, Baguley BC (2005). Disrupting tumour blood vessels. Nat Rev Cancer 5: 423–435.

Vacca A, Ribatti D, Presta M, Minischetti M, Iurlaro M, Ria R *et al*. (1999). Bone marrow neovascularization, plasma cell angiogenic potential, and matrix metalloproteinase-2 secretion parallel progression of human multiple myeloma. Blood 93: 3064–3073.

Vassal E, Barette C, Fonrose X, Dupont R, Sans-Soleilhac E, Lafanechere L (2006). Miniaturization and validation of a sensitive multiparametric cell-based assay for the concomitant detection of microtubule-destabilizing and microtubule-stabilizing agents. J Biomol Screen 11: 377–389.

Supporting information

Additional Supporting Information may be found in the online version of this article:

Figure S1 Reversibility of CM01 and CM02 effects in HeLa cells. HeLa cells were treated for 2 h with 0.25% DMSO (control); 5 μM colchicine; 10 μM nocodazole, 25 μM nocodazole, 25 μM CM01 or 25 μM CM02, as indicated. Compounds were the removed and cells were incubated overnight in fresh medium. They were then fixed and stained for α-tubulin.

Table S1 Flow chart of the automated screening of the library and the subsequent analysis of active compounds.

Appendix S1 Cell lines and culture.